Environmental Science: Atmospheres

ROYAL SOCIETY OF CHEMISTRY

PAPER

View Article Online
View Journal | View Issue

Cite this: *Environ. Sci.: Atmos.*, 2023, **3**, 1485

OH and Cl radicals initiated oxidation of amyl acetate under atmospheric conditions: kinetics, products and mechanisms

Vianni G. Straccia C.,[a] María B. Blanco[ab] and Mariano A. Teruel *[a]

The relative rate coefficients of the gas-phase reaction of amyl acetate, (AA), $CH_3COO(CH_2)_4CH_3$ with OH radicals and Cl atoms were determined at (298 ± 2) K and 1000 mbar of pressure. The experiments were developed in two different atmospheric Pyrex chambers coupled with "*in situ*" Fourier Transform Infrared (FTIR) spectroscopy and Gas Chromatography equipped with flame ionization detection (GC-FID). The rate coefficients obtained from the average of different experiments were (in units of cm^3 $molecule^{-1}$ s^{-1}): $k_{AA+OH\text{-}FTIR} = (6.00 \pm 0.96) \times 10^{-12}$; $k_{AA+OH\text{-}GC\text{-}FID} = (6.37 \pm 1.50) \times 10^{-12}$ and $k_{AA+Cl\text{-}GC\text{-}FID} = (1.35 \pm 0.14) \times 10^{-10}$. Additionally, product studies were completed for the Cl-initiated oxidation of AA, in similar conditions of the kinetic experiments by Gas Chromatography coupled with a mass detector (GC-MS) with Solid Phase Micro Extraction (SPME). Acetic acid, formaldehyde, acetaldehyde, propionaldehyde, and butyraldehyde were the main products identified. Complementary Structure Activity Relationships (SAR) were developed to compare with the experimental kinetic results and to clarify the individual reactivity sites of the ester. The atmospheric oxidation pathways of the AA are postulated and discussed taking into account the observed products and the SAR estimations. The initial pathway for the degradation of AA initiated by Cl atoms and OH radicals occurs *via* H-atom abstraction at $-C(O)OCH_2-$ (C1); $-CH_2-$ (C2); $-CH_2-$ (C3); and $-CH_2CH_3-$ (C4) moieties. The atmospheric implications of the reactions studied were evaluated by the estimation of their tropospheric lifetimes toward OH radicals and Cl atoms to be: $\tau_{OH} = 22$ and $\tau_{Cl} = 62$ hours. Consequently, the estimated average ozone production ($[O_3] = 2.15$) suggests a potential contribution of these compounds emission to the formation of photochemical smog. On the other hand, the Photochemical Ozone Creation Potential (POCP) for AA was calculated to be POCP = 70.2. A moderate risk of photochemical smog production suggests that this ester could be harmful to the health and the biota in urban environments.

Received 6th June 2023
Accepted 17th August 2023

DOI: 10.1039/d3ea00082f

rsc.li/esatmospheres

Environmental significance

Reactivity information, SAR estimations and free energy relationships, together with a detailed understanding of products and atmospheric pathways, is necessary for a thorough assessment of the atmospheric impact of saturated esters to the air. In this study, the rate coefficients of the amyl acetate oxidation, initiated by Cl atoms and OH radicals, were determined under quasi-real atmospheric conditions using different experimental methodology. The atmospheric lifetime of the saturated ester studied determines their contribution to the average ozone production. Furthermore, small aldehydes such as formaldehyde, acetaldehyde, propionaldehyde and butyraldehyde are products reaction and secondary pollutants, could affect air quality and other environmental compartments. Aldehydes, as highly reactive compounds in the atmosphere, can contribute to the atmospheric oxidation capacity as well as to the formation of tropospheric ozone and other photooxidants of the photochemical smog.

1 Introduction

The atmosphere is filled with Volatile Organic Compounds (VOCs), which are released from several anthropogenic or natural sources. Numerous VOCs can undergo photochemical reactions that result in the creation of ozone and other harmful byproducts when combined with sunlight radiation and molecular oxygen. These VOCs react with hydroxyl radicals (OH), which is the main atmospheric sink and where ozone or other products are formed. Additionally, other atmospheric oxidants, including Cl atoms, NO_3 radicals, and O_3 molecules could react with these VOCs.[1]

Acetates are a type of VOCs that are extensively utilized in various industrial procedures, primarily as solvents and in the production of fragrances and flavors. In nature, vegetation also

[a](L.U.Q.C.A), Laboratorio Universitario de Química y Contaminación del Aire, Instituto de Investigaciones en Fisicoquímica de Córdoba (I.N.F.I.Q.C.), Dpto. de Fisicoquímica, Facultad de Ciencias Químicas, Universidad Nacional de Córdoba, Ciudad Universitaria, 5000 Córdoba, Argentina. E-mail: mariano.teruel@unc.edu.ar; Fax: (+54) 351-4334188

[b]Institute for Atmospheric and Environmental Research, University of Wuppertal, DE-42097 Wuppertal, Germany

generates these substances.[2] AA is used as a cosmetic product, mainly in nail polishes, enamels, and lacquer. Additionally, it serves as a solvent in nail enamel remover and employed in inks, adhesives or thinners.[3]

The atmospheric oxidation of AA, which is most likely to be initiated by OH radicals or Cl atoms, may have an impact on the production of ozone and other photochemical smog byproducts in urban areas.

To assess the effects of anthropogenic and biological factors on air quality, it is necessary to combine kinetic data with mechanistic information about the overall oxidation process at atmospheric pressure and room temperature.

In the present work, we present relative rate coefficient data for the reactions of the OH radical and Cl atoms with AA at (298 ± 52) K and 1000 mbar of pressure, using *in situ* FTIR spectroscopy and GC-FID, as analytical techniques. In addition, product studies and SAR estimations were developed for the first time for the Cl-initiated oxidation of AA to postulate the atmospheric chemical mechanism of this ester at NO_x-free conditions.

The atmospheric lifetimes of AA were calculated using the experimental rate coefficients determined in this work to assess the potential consequences of the studied reactions on the atmosphere. The estimation of $[O_3]$ and POCP will assess the local, regional and/or global environmental implications of the reactions studied.

2 Experimental section

All the experiments were performed in a 405 L and 480 L Pyrex glass reactors at (298 ± 2) K and 1000 mbar = 1 atmosphere of pressure. A complete description of the reactor can be found elsewhere.[4] and only a brief explanation are given here. The chamber is composed of a cylindrical borosilicate glass vessel of 1.5 and 3 m. The reactors are surrounded by fluorescence lamps, which emit at a maximum of 360 nm. The radicals are produced by the radiation of the lamps. The 405 L reactor is coupled to a gas chromatograph equipped with flame ionization detection Shimadzu GC-2014B, using an Rtx-5 capillary column (fused silica G27, 30 m × 0.25 mm 0.25 μm) using SPME as a sampling method, the gray fiber is composed of Divinylbenzene/Carboxen/Polydimethylsiloxane (DVB/CAR/PDMS).

On the other hand, the 480 L reactor is coupled to an *in situ* Thermo Nicolet Nexus spectrometer brand equipped with a liquid nitrogen-cooled Mercury–Cadmium–Telluride (MCT) detector was used to observe the loss of the reactants, and the appearance of products. This reactor has a support system for multiple reflection mirrors type "White". This system lets many reflections inside the reactor grow the optical path, which allow us to work with lower concentrations of few ppm of VOCs of interest.

Using both reactors with different analytical techniques, the determination of the rate coefficients were performed by the relative method. With this method, the rate coefficient of AA could be determined indirectly from their relationship with the rate coefficient of a reference reaction. Therefore, AA and the reference compounds (ethylene, dimethyl ether, *Z*-1,2-dichloroethylene, and trichloroethylene) react with OH radicals or Cl atoms competitively as the following:

$$CH_3COO(CH_2)_4CH_3 + OH \text{ or } Cl \rightarrow \text{products} \quad (1)$$

$$\text{Reference compound} + OH \text{ or } Cl \rightarrow \text{products} \quad (2)$$

OH radicals were generated by photolysis of H_2O_2 at 254 nm as follows:

$$H_2O_2 + h\nu\ (\lambda\text{-}254\ \text{nm}) \rightarrow 2OH \quad (3)$$

Cl atoms were generated by UV photolysis of oxalyl chloride (ClCOCOCl) and/or Cl_2

$$Cl_2 + h\nu\ (\lambda\text{-}360\ \text{nm}) \rightarrow 2Cl \quad (4)$$

$$ClC(O)C(O)Cl + h\nu\ (\lambda\text{-}254\ \text{nm}) \rightarrow 2Cl + 2CO \quad (5)$$

Considering that reactions (1) and (2) are the only reactions that consume the reactants, it is possible to determine the relative rate coefficient of the reactions of interest as:

$$\ln\left[\frac{[AA]_0}{[AA]_t}\right] = \frac{k_{AA}}{k_{ref}} \ln\left[\frac{[ref]_0}{[ref]_t}\right] \quad (6)$$

where $[ref]_0$, $[ref]_t$, $[AA]_0$, and $[AA]_t$ are the concentrations of the reference compound and AA at times $t = 0$ and t, respectively. The slope of plots of eqn (6) is the relationship between the rate coefficient of the reference compound and AA.

Previous tests were carried out to check that reactions (1) and (2) were the only ones that occur significantly inside the reactor. To ensure any reactions between them, the tests involved combining specified quantities of AA with various reference compounds. These mixtures were then exposed to the lamps to check the photolysis of the compound. Furthermore, no reactions between the compounds and radical's precursor in the dark were detected.

For product studies, mixtures of AA with oxidants in synthetic air/N_2 were irradiated; in a similar condition as in the kinetic study. We used GC-MS to identify the products reaction. In addition, the products were monitored with a GC-MS VARIAN Saturn 2200 with column HP-5MS, Agilent (Part 19091S-433) of 30 meters in length, 0.25 mm internal diameter and film thickness 0.25 μm. The following sampling techniques were used to take gas samples from the chamber: (a) the SPME was treated to derivatization using O-((perfluorobenzyl) methyl) hydroxylamine (PFBHA). For this, the microfiber was exposed for 2 minutes for headspace extraction to the derivatizing agent solution. After the SPME covered with PFBHA was exposed to the chamber with the gas reaction for 5 minutes before being injected into the GC-MS at 220 °C. (b) The SPME was exposed for 10 minutes to the gas reaction by the pre-concentration method followed by the injection into the GC-MS for 2 minutes at 180 °C.

The initial concentrations (in ppm) used in the experiments were for AA (3) by FTIR and (6) by GC-FID, (2.4) for ethylene, (2.4) for dimethyl ether, (8) for *Z*-1,2-dichloroethylene, (7) for

trichloroethylene, (77) for hydrogen peroxide. (1 ppm = 2.46 × 10^{13} molecule cm^{-3} at 298 K and 760 torr of total pressure).

The chemicals used in the experiments had the following purities as given by the manufacturer and were used as supplied: nitrogen (air liquid 99.999%), synthetic air (air liquid, 99.999%), Cl_2 (Messer Griesheim, 2.8), amyl acetate (Sigma-Aldrich, ≥99%), ethylene (Sigma-Aldrich, ≥99.5%), dimethyl ether (Sigma-Aldrich, 99%), *Z*-1,2-dichloroethylene (Sigma-Aldrich, 97%), trichloroethylene (Supelco, 98%), and hydrogen peroxide (Interox, 85% w/w).

3 Results and discussion

3.1 Kinetics

The rate coefficients for the reactions studied (1) and (2) were determined employing eqn (6) with different reference compounds for each technique as follows:

$$\text{FTIR } C_2H_4 + OH \rightarrow \text{products} \quad (7)$$

$$\text{FTIR } C_2H_6O + OH \rightarrow \text{products} \quad (8)$$

$$\text{GC-FID } C_2HCl_3 + OH \rightarrow \text{products} \quad (9)$$

$$\text{GC-FID } Z\text{-}C_2H_2Cl_2 + OH \rightarrow \text{products} \quad (10)$$

$$\text{GC-FID Z-}C_2H_2Cl_2 + Cl \rightarrow \text{products} \quad (11)$$

$$\text{GC-FID } C_2HCl_3 + Cl \rightarrow \text{products} \quad (12)$$

where k_7 (ref. 5) = (9.00 ± 0.30) × 10^{-12}; k_8 (ref. 6) = (2.77 ± 0.07) × 10^{-12}; k_9 (ref. 7) = (2.23 ± 0.10) × 10^{-12}; k_{10} (ref. 8) = (2.38 ± 0.14) × 10^{-12}; k_{11} (ref. 9) = (9.65 ± 0.10) × 10^{-11}; k_{12} (ref. 9) = (8.08 ± 0.10) × 10^{-11}. All the *k* values are in units of cm^3 $molecule^{-1}$ s^{-1}.

The rate coefficients for the reaction under study with two oxidants were determined by the performance of at least two experiments. Fig. 1a–c show the plots $\ln[AA]_0/[AA]_t$ *versus* $\ln[\text{reference}]_0/[\text{reference}]_t$ of two or three samples for each reference compound for the OH initiated reactions. **1a** Shows the plots obtained by the FTIR technique developed using N_2 with ethene and dimethyl ether as reference compounds. **1b** and **1c** shows the plots obtained by the GC-FID technique using synthetic air as a gas bath with trichloroethylene and *Z*-1,2-dichloroethylene as reference compounds, respectively.

All plots show linearity of the straight lines obtained, with correlation coefficients close to 1 and nearly zero intercepts indicating that secondary reactions are negligible.

Fig. 2 shows plots obtained for the reaction of AA with Cl atoms. **2a** shows the plots of three experiments performed using trichloroethylene as reference compounds and **2b** shows the plots obtained using *Z*-1,2-dichloroethylene as reference compounds.

Table 1 lists the rate coefficients for the reaction of each reference compound with both oxidants. It also includes the ($k_{AA}/k_{reference}$) ratios obtained from measurements conducted using both oxidants and techniques, along with the corresponding rate coefficient values in absolute terms. These rate

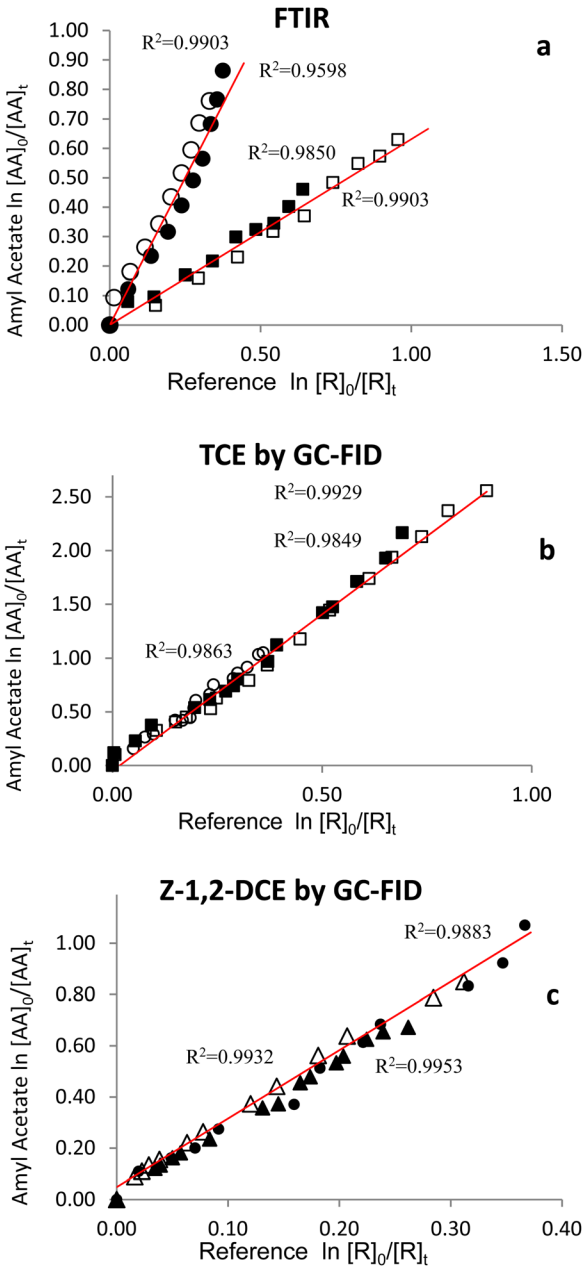

Fig. 1 Kinetic data for the reaction of AA with OH radicals obtained at 298 K and atmospheric pressure with (a) FTIR technique using ethene (R1 □ and R2 ■) and dimethyl ether (R1 ○ and R2 ●) and (b) GC-FID technique using trichloroethylene (R1 □, R2 ■, and R3 ○) and (c) *Z*-1,2-dichloroethylene (R1 ▲, R2 △, and R3 ●) as reference compounds.

coefficient ratios are each from the average of two or three measurements. The value of the photolysis rate for AA is also included. This value was used to correct the final value of the rate coefficient for each reaction.

Table 1 shows that there is good agreement between the results obtained using two different simulation chambers, four different reference compounds and *in situ* FTIR and GC-FID as detection methods. The following are the recommended average rate coefficients:

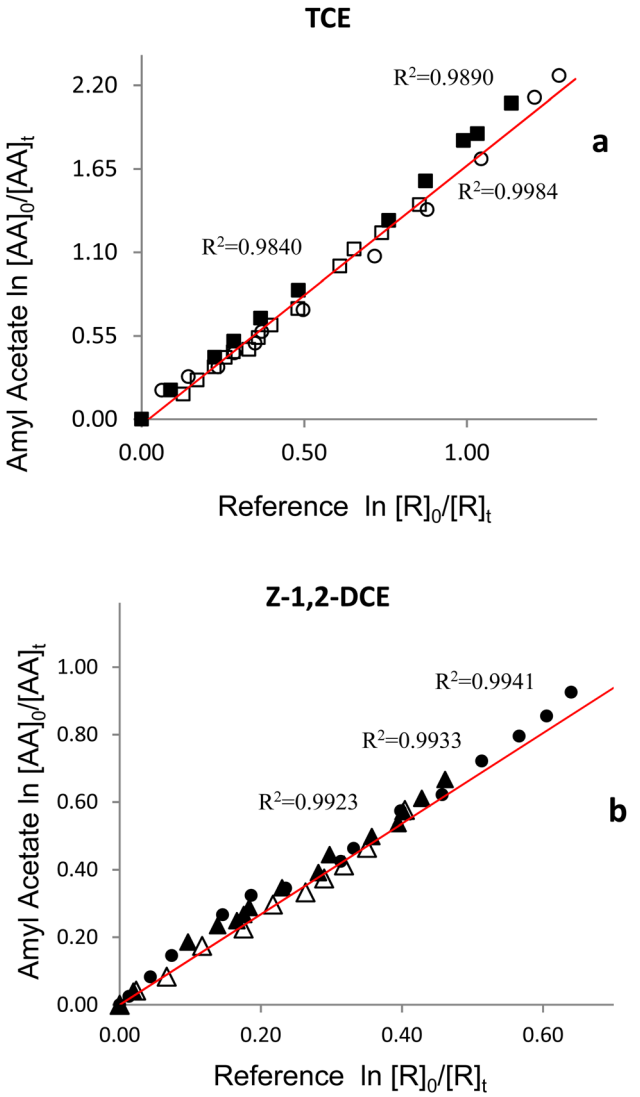

Fig. 2 Kinetic data for the reaction of AA with (ClC(O)C(O)Cl) as precursor of Cl atoms obtained at 298 K and atmospheric pressure with GC-FID technique using (a) trichloroethylene (R1 □, R2 ■, and R3 ○) and (b) *Z*-1,2-dichloroethylene (R1 ▲, R2 △, and R3 ●) as reference compounds.

$$k_{\mathrm{AA+OH\text{-}FTIR}} = (6.00 \pm 0.96) \times 10^{-12}\ \mathrm{cm^3\ molecule^{-1}\ s^{-1}}$$

$$k_{\mathrm{AA+OH\text{-}GC\text{-}FID}} = (6.37 \pm 1.50) \times 10^{-12}\ \mathrm{cm^3\ molecule^{-1}\ s^{-1}}$$

$$k_{\mathrm{AA+Cl\text{-}GC\text{-}FID}} = (1.35 \pm 0.14) \times 10^{-10}\ \mathrm{cm^3\ molecule^{-1}\ s^{-1}}$$

The errors shown are twice the standard deviation that results from the least-squares fit of the straight lines. The corresponding error has also been considered in the reference rate coefficients of the reaction.

The values of the rate coefficients of reactions with OH radicals are found to be fairly similar between 2 different detection techniques, *in situ* infrared spectroscopy and gas chromatography with sample extraction by SPME.

For comparison purposes, the rate coefficient for the reaction of AA with OH radicals was estimated from the Structure–Activity Relationships (SAR). The rate coefficient calculation software (US Environmental Protection Agency), AOPWIN[10] v.4.11 was used, based on the method developed by Kwok and Atkinson (1995).[11] The rate coefficient calculated for H-abstraction was 6.02×10^{-12} cm^3 molecule^{-1} s^{-1}. It is shown a good concordance between the estimated rate coefficients values by SAR calculations and the obtained experimentally by FTIR $(6.00 \pm 0.96) \times 10^{-12}$ cm^3 molecule^{-1} s^{-1} and by GC-FID $(6.37 \pm 1.50) \times 10^{-12}$ cm^3 molecule^{-1} s^{-1}.

Furthermore, there are previous kinetic data reported for the reactions of OH radicals with AA, performed with pulsed Laser Photolysis Laser Induced Fluorescence technique (PLP-LIF), where it can be possible to compare with our relative determination in atmospheric conditions. The authors reported the absolute value[2] of $(7.34 \pm 0.91) \times 10^{-12}$ cm^3 molecule^{-1} s^{-1}. On the other hand, Williams *et al.* 1993, reported relative values for the rate coefficient of AA with OH radicals using Gas Chromatography with Flame Ionization Detection[12] of: $(7.53 \pm 0.48) \times 10^{-12}$ cm^3 molecule^{-1} s^{-1}. Additionally, previous kinetic study of AA with OH radicals reaction are reported in a doctoral theses[13] by Zogka, 2016. In that theses, values of $k_{\mathrm{AA+OH+1,3\text{-}dioxolane}} = (6.96 \pm 0.27) \times 10^{-12}$ cm^3 molecule^{-1} s^{-1} and $k_{\mathrm{AA+OH+1\text{-}pentanol}} = (7.61 \pm 0.33) \times 10^{-12}$ cm^3 molecule^{-1} s^{-1}, were determined using relative technique and atmospheric simulation chamber of Teflon coupled to GC-FID. Although, there are small differences within the experimental errors, the agreement between the data obtained in this work by GC-FID and by *in situ* FTIR with the previous relative GC-FID and PLP-LIF values is reasonable, taking into account the experimental errors of all determinations.

Additionally, the predicted rate coefficient for the reaction of AA with Cl atoms was also evaluated using the SAR method. This method was first developed to study how alkanes react with Cl atoms, but it has been modified to take additional functional groups in more complex compounds into account.[14] This method consists of computing the overall rate coefficient based on the estimation of the rate coefficient for H-abstraction atoms from the groups –CH_3, –CH_2– and >CH– for the interaction of Cl atoms with alkanes.[15]

The group rate coefficients just consider the identity of the substituents next to the alkyl moiety as follow:

$$k\ (\mathrm{CH_3}\text{–}X) = k_{\mathrm{prim}}\ F(X),$$

$$k\ (X\text{–}\mathrm{CH_2}\text{–}Y) = k_{\mathrm{sec}}\ F(X)\ F(Y),$$

$$k\ (X\text{–CH–}Y(Z)) = k_{tert}\ F(X)\ F(Y)\ F(Z)$$

where, $k_{\mathrm{prim}} = 3.32$, $k_{\mathrm{sec}} = 8.34$, $k_{tert} = 6.09$ all k in unit of ($\times 10^{-11}$ cm^3 molecule^{-1} s^{-1}). $F(X)$ $F(Y)$ $F(Z)$ are the moieties factor of the substituent groups X, Y, and Z, respectively.[16] The SAR values were calculated using the available substituent factors reported in many studies. Table 2 presents the factor for each moiety compiled according to the structure of the AA, $CH_3COO(CH_2)_4CH_3$.

Table 1 Rate coefficient ratios $k_{AA}/k_{reference}$, $k_{photolysis}$, rate coefficients for the reactions of OH radicals and Cl atoms with AA using different reference compounds at (298 ± 2) K in 760 Torr of pressure

	$k_{photolysis\ AA} \times s^{-1}$	Technique	Reference compound	$k_{reference} \times 10^{12}$	$k_{AA}/k_{reference}$	$k_{AA} \times 10^{12}$ cm^3 molecule^{-1} s^{-1}
AA + OH	5.29×10^{-5}	FTIR	C_2H_4	9.00 ± 0.30	0.66 ± 0.04	5.94 ± 0.55
					0.68 ± 0.02	6.12 ± 0.39
			C_2H_6O	2.77 ± 0.07	2.15 ± 0.16	5.96 ± 0.59
					2.16 ± 0.07	5.98 ± 0.34
					Average	6.00 ± 0.96
	2.42×10^{-3}	GC-FID	C_2HCl_3	2.23 ± 0.10	2.90 ± 0.18	6.47 ± 0.69
					2.91 ± 0.14	6.49 ± 0.60
					2.89 ± 0.09	6.44 ± 0.49
			Z-$C_2H_2Cl_2$	2.38 ± 0.14	2.59 ± 0.10	6.16 ± 0.60
					2.67 ± 0.14	6.36 ± 0.70
					2.65 ± 0.11	6.31 ± 0.63
					Average	6.37 ± 1.50
	$k_{photolysis\ AA} \times s^{-1}$	Technique	Reference compound	$k_{reference} \times 10^{11}$	$k_{AA}/k_{reference}$	$k_{AA} \times 10^{10}$ cm^3 molecule^{-1} s^{-1}
AA + Cl	2.27×10^{-3}	GC-FID	C_2HCl_3	8.08 ± 0.10	1.82 ± 0.02	1.47 ± 0.03
					1.63 ± 0.06	1.32 ± 0.07
					1.71 ± 0.05	1.38 ± 0.06
			Z-$C_2H_2Cl_2$	9.65 ± 0.10	1.36 ± 0.06	1.31 ± 0.07
					1.34 ± 0.04	1.28 ± 0.05
					1.37 ± 0.05	1.32 ± 0.06
					Average	1.35 ± 0.14

From the data presented in Table 2 the following SAR value for the reaction of AA with Cl atoms has been estimated: 2.05×10^{-10} cm^3 molecule^{-1} s^{-1}. It should be observed that the estimated rate coefficients value and the experimentally measured of $(1.35 \pm 0.14) \times 10^{-10}$ cm^3 molecule^{-1} s^{-1} are close considering the experimental error.

Moreover, there are previous kinetic data reported by Zogka, 2016 (ref. 13) for the reactions of AA with Cl atoms. Values reported were $k_{AA+Cl+n\text{-pentane}} = (2.07 \pm 0.04) \times 10^{-10}$ cm^3 molecule^{-1} s^{-1} and $k_{AA+Cl+1\text{-butanol}} = (2.13 \pm 0.03) \times 10^{-10}$ cm^3 molecule^{-1} s^{-1}. The values reported by us could be slightly lower than those reported by Zogka. However, there is another value reported by Ifang *et al.* 2015. The rate coefficient informed[14] of $(1.790 \pm 0.153) \times 10^{-10}$ cm^3 molecule^{-1} s^{-1} is also in agreement with the value reported in this work.

A previous reaction trend reported by Atkinson 1986 (ref. [18]) for acetates pointed out that the rate coefficient for the reaction of acetates with OH radicals increases with the length of the carbon chain. The following rate coefficient values have been reported in several studies: $CH_3C(O)OCH_3$, $k_{(methyl\ acetate+OH)}$[19] = 3.5×10^{-13}; $CH_3C(O)OCH_2CH_3$, $k_{(ethyl\ acetate+OH)}$[20] = 1.73×10^{-12}; $CH_3C(O)OCH_2CH_2CH_3$, $k_{(propyl\ acetate+OH)}$[21] = 1.97×10^{-12}; $CH_3C(O)OCH_2CH_2CH_2CH_3$, $k_{(butyl\ acetate+OH)}$[22] = 5.20×10^{-12}; $CH_3C(O)OCH_2CH_2CH_2CH_2CH_3$, $k_{(AA+OH)-average\ this\ work} = 6.19 \times 10^{-12}$, all the k values are in units of cm^3 molecule^{-1} s^{-1}. That is the k_{OH} increase with the number of secondary (CH_2) and tertiary (C–H) bonds. On the other hand, there is a similar trend for the reactions of acetates with Cl atoms. Several research have reported the corresponding rate coefficient values for the Cl atoms as follows: $CH_3C(O)OCH_3$, $k_{(methyl\ acetate+Cl)}$[23] = 2.20×10^{-12}; $CH_3C(O)OCH_2CH_3$, $k_{(ethyl\ acetate+Cl)}$[14] = 1.71×10^{-11}; $CH_3C(O)OCH_2CH_2CH_3$, $k_{(propyl\ acetate+Cl)}$[14] = 7.70×10^{-11}; $CH_3C(O)OCH_2CH_2CH_2CH_3$, $k_{(butyl\ acetate+Cl)}$[14] = 1.20×10^{-10}; $CH_3C(O)OCH_2CH_2CH_2CH_2CH_3$, $k_{(AA+Cl)-average\ this\ work} = 1.35 \times 10^{-10}$, all the k values are in units of cm^3 molecule^{-1} s^{-1}. Similar to the reaction with OH radicals, the rate coefficient for the reaction of acetates with Cl atoms increases with the length of the carbon chain. The values obtained in this work are consistent with the trend reported. There is the first experimental kinetic study of the reaction of AA with Cl atoms using the relative kinetic technique in a photoreactor coupled to FTIR spectrometers.[14]

Table 2 SAR group reactivity factors for the reaction with Cl atoms

Substituent	Factor (Cl)	Ref.
(–C(O)OR)	0.12	Ifang *et al.*, 2015 (ref. 14)
(RC(O)O–)	0.066	Xing *et al.*, 2009 (ref. 17)
($-CH_3$)	1	Aschmann and Atkinson[16]
($-CH_2-$)	0.79	

3.2 Free energy relationships

Several studies found a linear relationship between the rate coefficients of different compounds in reaction with OH radicals and Cl atoms.[24,25] In this study, Table 3 shows a relationship between k_{OH} and k_{Cl} of several esters and ketones reported previously in the literature, including the kinetic data for AA from the present determination. The relationship between the rate coefficients for the reactions of OH radicals and Cl atoms is presented in Fig. 3 where a significant correlation is established. The data from Fig. 3 are subjected to a least-squares analysis, which produces the following expression:

Table 3 Comparison between k_{OH} and k_{Cl} of a series of esters and ketones, together with the kinetic data for AA obtained in this work, at (296 ± 2) K

Compound	k_{Cl} (cm^3 molecule^{-1} s^{-1})	Ref. Cl	k_{OH} (cm^3 molecule^{-1} s^{-1})	Ref. OH
Methyl acetate	2.20×10^{-12}	23	3.20×10^{-13}	2
Ethyl acetate	1.71×10^{-11}	14	1.67×10^{-12}	2
Propyl acetate	7.70×10^{-11}	14	3.42×10^{-12}	2
Butyl acetate	1.20×10^{-10}	14	5.52×10^{-12}	2
Amyl acetate	1.35×10^{-10}	This work	6.19×10^{-12}	This work
Methyl butanoate	4.77×10^{-11}	26	3.29×10^{-12}	26
Methyl pentanoate	7.84×10^{-11}	26	5.02×10^{-12}	26
Methyl-2-methyl-butanoate	9.41×10^{-11}	26	3.78×10^{-12}	26
Methyl propanoate	1.68×10^{-11}	14	8.30×10^{-13}	27
Ethyl propanoate	4.19×10^{-11}	14	2.14×10^{-12}	28
Propyl propanoate	9.84×10^{-11}	14	4.40×10^{-12}	29
Ethyl butyrate	1.00×10^{-10}	29	5.70×10^{-12}	29
Methyl isobutyrate	4.20×10^{-11}	29	2.00×10^{-12}	29
2-Pentanone	1.11×10^{-10}	30	4.74×10^{-12}	31
3-Pentanone	8.10×10^{-11}	30	1.85×10^{-12}	31
2-Hexanone	1.88×10^{-10}	30	9.16×10^{-12}	31
3-Hexanone	1.43×10^{-10}	30	6.96×10^{-12}	31
Butanone	4.04×10^{-11}	30	1.04×10^{-12}	32

$$\log k_{OH} = 1.1294 \log k_{Cl} - 0.0123 \ (r^2 = 0.99) \quad (13)$$

There is a direct relationship between the rate coefficients for both oxidants as it can be seen in the free energy plot for the various oxygenated compounds.

The good quality of the correlation between the reaction rate coefficients of OH radicals and Cl atoms is such that an estimation of the rate coefficients can be made for reactions which have not yet been investigated. In addition, this correlation shows that the degradation mechanism initiated by the Cl atoms is similar that OH radicals, *i.e.*, by the abstraction of the H atoms.

3.3. Products studies

Mixtures of AA with molecular chlorine in air were photolyzed to identify the oxidation products. These experiments were conducted under similar conditions to the kinetic experiments. Approximately 50% of consumption the original ester concentration was used in the development of each study.

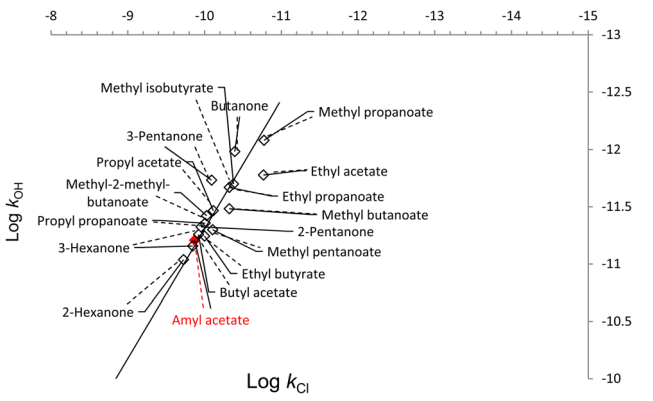

Fig. 3 Free energy plots log(k_{OH}) *vs.* log(k_{Cl}) for the reactions with Cl and OH of esters and ketones reported in previous work together with the AA studied in this work (Table 3).

The atmospheric degradation of saturated esters with atmospheric oxidants is initiated by H-atoms abstraction from the alkyl groups CH; CH_2; and/or CH_3. This produces alkyl radicals with the following stability trend[33] being CH > CH_2 > CH_3. The abstraction of H-atoms will be based on SAR estimated probability as follows; 0.7% at –CH_3C(O)O–; 30% at –C(O)OCH_2– (C_1); 23% at –CH_2– (C_2); 23% at –CH_2– (C_3); 19% at –CH_2CH_3– (C_4); and 3% at –CH_3 (C_5). These probabilities obtained from SAR estimation proposed that there will be several routes and secondary carbons will be the main pathway of H-atom abstraction.

GC-MS studies were developed to identify the end products of the chemical reaction between AA and Cl atoms. The SPME (DVB/CAR/PDMS) microfiber was exposed in the PFBHA before being exposed to the gas reaction in the Pyrex chamber. The products, formaldehyde, acetaldehyde, propionaldehyde, and butyraldehyde were positively identified as carbonyl oximes due to the reaction with the PFBHA (see Fig. 4 and 5). The following carbonyl oximes were found: formaldehyde oxime, *o*-[(pentafluorobenzyl) methyl]; acetaldehyde oxime, *o*-[(pentafluorobenzyl) methyl]; propionaldehyde oxime, *o*-[(pentafluorobenzyl) methyl]; and butyraldehyde oxime, *o*-[(perfluorobenzyl) methyl]. Acetic acid was found without derivatizing on the experiments by the pre-concentration method.

The mixture was photolyzed using air as bath gas and AA was detected at a retention time of 4.6 min with the matching (*m*/*z*) ratios of 43, 55, 70, 87 and 115 (see Fig. 4 and 5). The particular fragments (*m*/*z*) of the main products at the successive retention times and the percentage of coincidence (match) are also shown in Fig. 5: formaldehyde at 11.7 min, (*m*/*z*): 47, 61, 81, 99, 117, 131, 161, 167, 181, and 225, with a match = 97%; acetaldehyde at 12.9 min, (*m*/*z*): 58, 81, 99, 117, 131, 161, 167, 181, 209, and

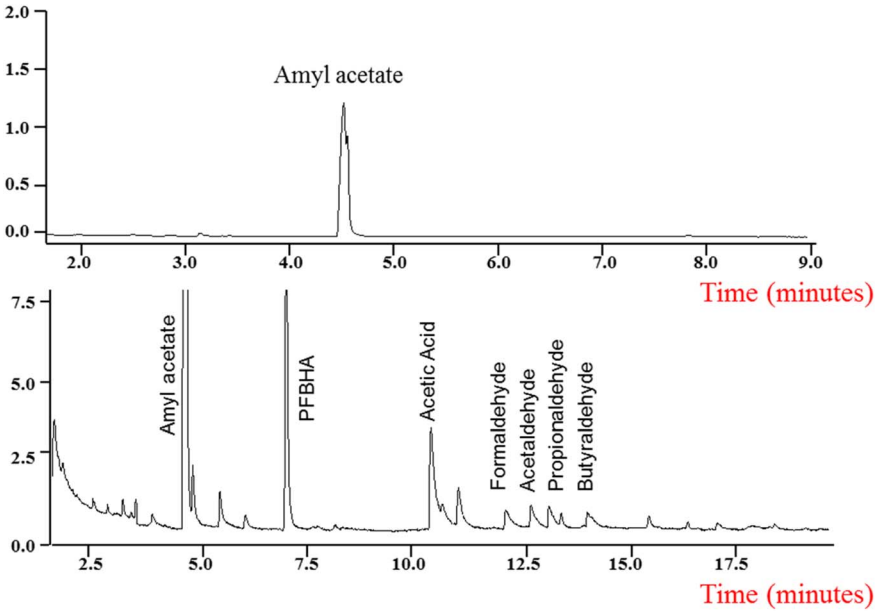

Fig. 4 GC-MS chromatogram of mixture of (AA + Cl_2) on air, before and after photolysis.

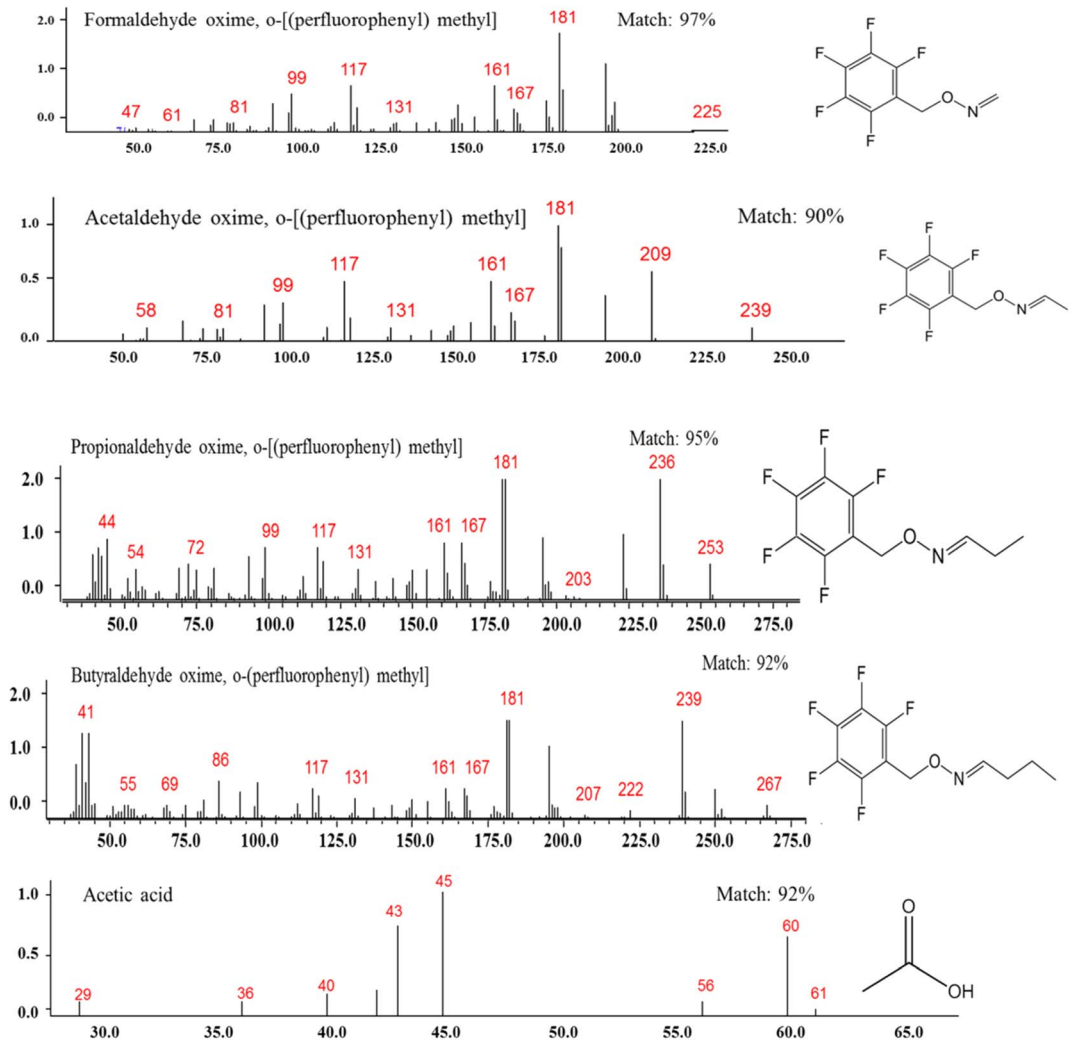

Fig. 5 Products observed and the mass spectra for formaldehyde, acetaldehyde, propionaldehyde, butyraldehyde and acetic acid.

239, with a match = 90%; propionaldehyde at 13.2 min, (*m*/*z*): 44, 54, 72, 99, 117, 131, 161, 167, 181, 203, 236, and 253, with a match = 95%; butyraldehyde at 14 min, (*m*/*z*): 41, 55, 69, 86, 117, 131, 161, 167, 181, 207, 222, 239, and 267, with a match = 92%; and acetic acid at 10.3 min, (*m*/*z*): 29, 36, 40, 43, 45, 56, 60, and 61, with a match = 92%. All of these fragments *m*/*z* are characteristic of these identified compounds.[34]

We postulate a degradation mechanism in Schemes 1 and 2 with four potential pathways, taking into account the products found and the SAR estimations of the reactive sites of AA.

Scheme 1 shows that the reaction between Cl atoms and AA can occur *via* H-atom abstraction at the $-C(O)OCH_2-$, (C_1), in channel A and from $-CH_2-$ (C_2) in channel B.

From channel A, the H-atoms abstraction from C_1 produces the alkyl radical $CH_3C(O)OC(^{\bullet})H(CH_2)_3CH_3$ followed by O_2 addition to form the peroxy radicals $CH_3C(O)OC(OO^{\bullet})H(CH_2)_3CH_3$ with further alkoxy radicals formation ($CH_3C(O)OC(O^{\bullet})H(CH_2)_3CH_3$). These $CH_3C(O)OC(O^{\bullet})H(CH_2)_3CH_3$ radicals can follow two different reaction pathways: (1) decomposition, with a C_1–C_2 bond cleavage producing a stable product, acetic formic anhydride, $CH_3C(O)OC(O)H$, and $^{\bullet}CH_2CH_2CH_2CH_3$ radicals. Further, these radicals will react with O_2 to form peroxy radicals eventually forming butyraldehyde, which was positively identified. (2) Can go through α-ester rearrangement and then a C–O scission, which occurred when the H-atom abstraction is from the carbon linked to the non-carbonyl oxygen to produce a carboxylic acid and the corresponding radical coproduct. Acetic acid was identified. The $^{\bullet}C(O)(CH_2)_3CH_3$ radicals react with O_2 to lead carbon dioxide and $^{\bullet}CH_2CH_2CH_2CH_3$ radicals. These radicals will finally form butyraldehyde.

On the other hand, channel B shows the H-atoms abstraction from the $-CH_2-$ (C_2). This H abstraction generates the alkyl radical $CH_3C(O)OCH_2C(-)HCH_2CH_2CH_3$ followed by O_2 addition to form the peroxy radicals $CH_3C(O)OCH_2C(OO^{\bullet})HCH_2CH_2CH_3$ and the corresponding alkoxy radical, $CH_3C(O)OCH_2C(O^{\bullet})HCH_2CH_2CH_3$. These alkoxy radicals can suffer scission. If the scission occurs between C_1–C_2, butyraldehyde, $CHOCH_2CH_2CH_3$ is produced together with $CH_3C(O)OC(^{\bullet})H_2$ radicals. These radicals react with O_2 followed by C_1–O cleavage to produce formaldehyde and CO_2. In contrast, if the scission occurs between C_2–C_3, 2-oxoethyl acetate, $CH_3C(O)OCH_2C(O)$ is produced with $^{\bullet}CH_2CH_2CH_3$ radicals as coproduct. The $^{\bullet}CH_2CH_2CH_3$ radicals will form, propionaldehyde, $CHOCH_2CH_3$.

Additionally, Scheme 2 shows two possible pathways. If the H-atoms abstraction is on the $-CH_2-$ (C_3), channel C, produced the radical $CH_3C(O)OCH_2CH_2C(^{\bullet})HCH_2CH_3$ followed by O_2 addition to form the alkoxy radical $CH_3C(O)OCH_2CH_2C(O^{\bullet})HCH_2CH_3$. These radicals can suffer scission. If the scission occurs between C_2–C_3 it is formed propionaldehyde, $CHOCH_2CH_3$, and $CH_3C(O)OCH_2C(^{\bullet})H_2$ radicals. These radicals will produce formaldehyde, CH_2O, and CO_2. If the scission occurs between C_3–C_4 will produce the stable compound $CH_3C(O)OCH_2CH_2C(O)H$, 2-oxo-2-(3-oxopropoxy)ethan-1-ylium, and $^{\bullet}CH_2CH_3$ radicals. The ethyl radicals produce acetaldehyde, $CHOCH_3$.

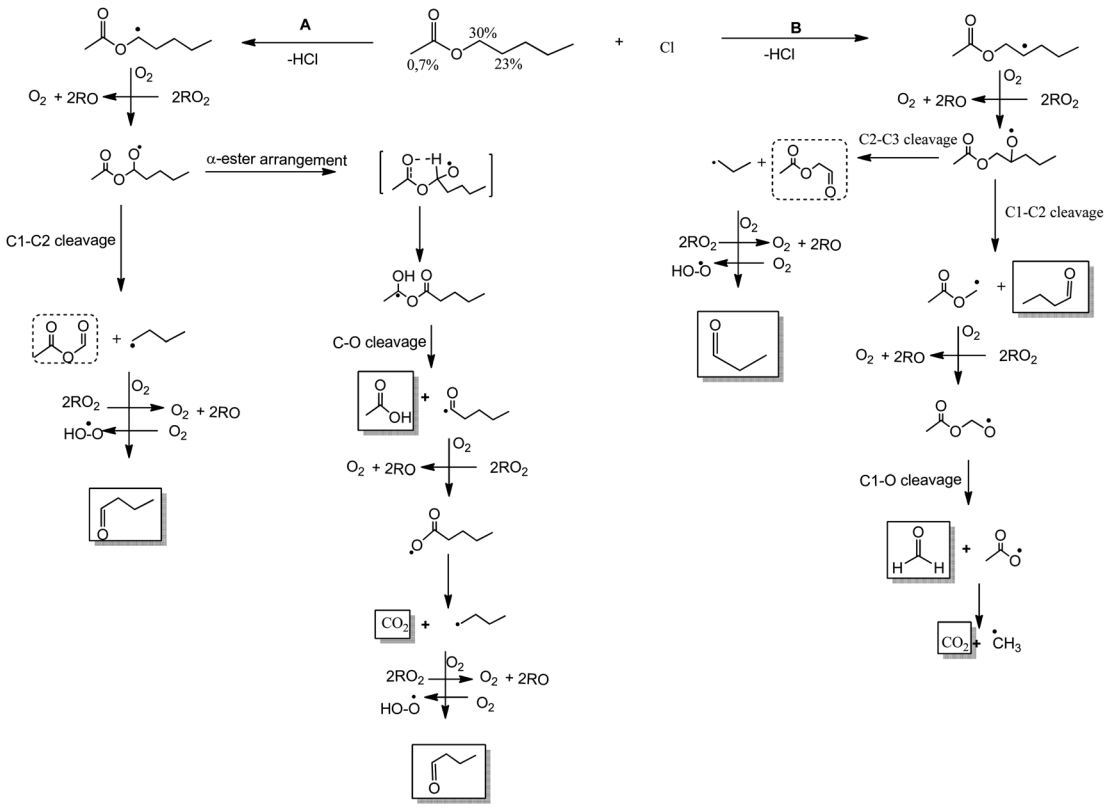

Scheme 1 Mechanism of Cl-atoms initiated oxidation of AA *via* H-abstraction from C_1 (channel A) and C_2 (channel B). Products identified in full line and unidentified products in dotted line.

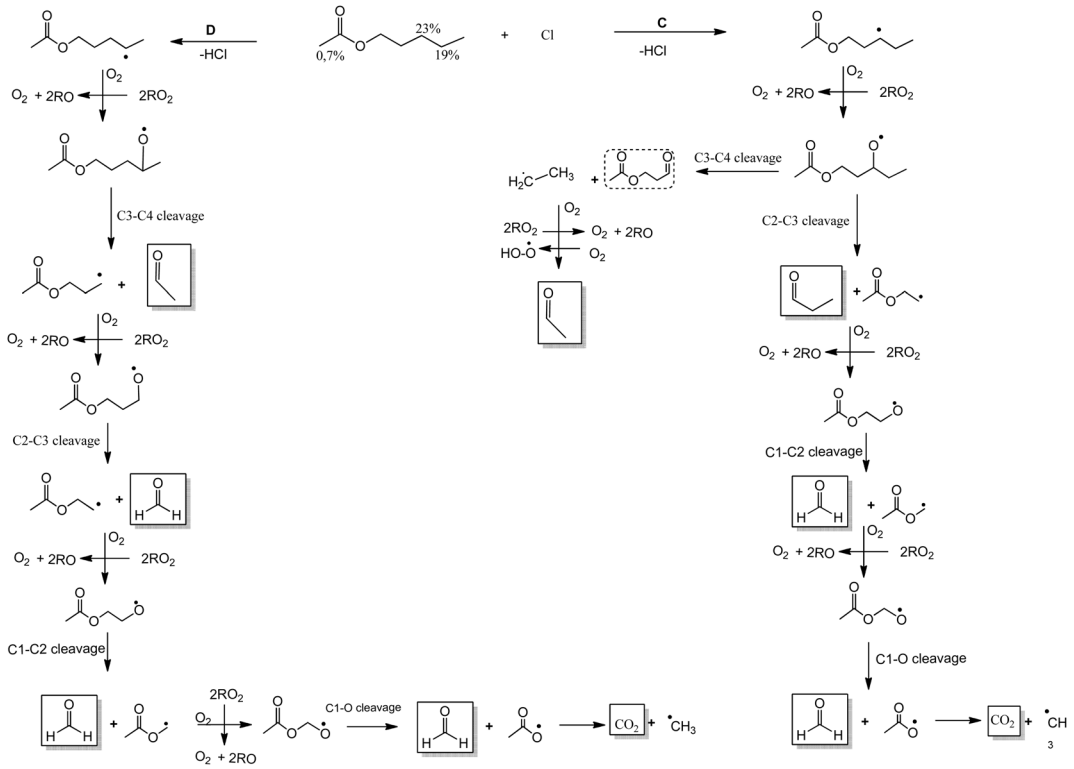

Scheme 2 Mechanism of Cl-atoms initiated oxidation of AA *via* H-abstraction from C_3 (channel C) and C_4 (channel D). Products identified in full line and unidentified products in dotted line.

If the H-atoms abstraction is on the $-CH_2-$ (C_4), (channel D), will form the radical $CH_3C(O)OCH_2CH_2CH_2C(^{\bullet})HCH_3$ followed by O_2 addition to form the alkoxy radical $CH_3C(O)OCH_2CH_2$-$CH_2C(O^{\bullet})HCH_3$. These radicals can undergo a cleavage between C_3–C_4 to lead to a stable compound, acetaldehyde, $CHOCH_3$, and $CH_3C(O)OCH_2CH_2C(^{\bullet})H_2$ radicals. These radicals could decompose to form formaldehyde and other radicals that will produce formaldehyde and CO_2.

The SAR calculations predict that channel A will be the primary reaction pathway (30%), followed by channels B and C (23%). Further studies will be necessary in order to quantify the product yields at various conditions, such as the presence or absence of NO_x, together with molecular theoretical research, in order to fully clarify the oxidation mechanism in different atmospheric scenarios.

As far as we are aware, no previous investigations have been performed concerning the products of AA and Cl atoms or with other tropospheric oxidants. Consequently, this is the first product distribution analysis of the mentioned reactions. The obtained product distribution and the proposed mechanism are consistent with the previously described pathways for the OH and Cl-initiated degradation of other saturated esters.[35]

4 Atmospheric chemistry implications

The rate coefficients of oxidation reactions with tropospheric oxidants such as OH radicals, Cl atoms, O_3 molecules, or NO_3 radicals and the average tropospheric oxidant concentrations can be used to calculate the tropospheric residence time (τ) by the expression $\tau = 1/k_{AA} \times$ [oxidants]. Where [OH] is 2.0×10^6 radicals cm^{-3} for about 12 hours (ref. 36) and [Cl] is $(3.3 \pm 1.1) \times 10^4$ atoms cm^{-3} for 24 hours.[37]

From Table 4, the values estimated are $\tau_{OH} = 22$, and $\tau_{Cl} = 62$ hours. The short lifetime for AA in the range of just over a few hours implies that the emission of this compound is likely to be removed rapidly in the gas phase close to its source of emission.

Unfortunately, there are no kinetic data available in the literature for the reactions of this compound with O_3 molecules, and NO_3 radicals with AA. Propyl acetate reacts with NO_3 with a rate coefficient of $(5.0 \pm 2.0) \times 10^{-17}$ cm^3 $molecule^{-1}$ s^{-1} according to reported data.[38] It may be predicted that the rate coefficient for AA should be on that order of magnitude with very small contribution as atmospheric sink of this ester by reaction with NO_3 radicals. AA was stable to actinic radiation according to previous photolysis investigations carried out before the kinetics experiments. These studies also did not demonstrate a significant decrease in the signals of the FTIR.

Due to the atmospheric lifetime, AA will probably contribute to ozone formation in local emission areas. For this reason, the POCP, was estimated using the modeling technique described by Jenkin *et al.*, 2017, with eqn (14), to evaluate the possible contribution of AA to the POCP.

$$\mathrm{POCP} = (A \times \gamma_S \times R \times S \times F) + P + R_{O_3} - Q \qquad (14)$$

where, A, γ_S, R, and S are core parameters used for all VOCs, F, P, R_{O_3} and Q are parameters used for specific groups of

Table 4 Atmospheric implications of AA

Reaction	$k_{average}$ cm^3 molecule^{-1} s^{-1}	τ (h)	$[O_3]^a$ (ppm)	POCP^b
AA + OH	$(6.19 \pm 1.23) \times 10^{-12}$	22	2.15	70.2
AA + Cl	$(1.35 \pm 0.14) \times 10^{-10}$	62		

^{a} Reference compounds: $CH_2 = CH_2 = 3.30$ ppm. ^{b} Reference compounds: $CH_2 = CH_2 = 100$.

compounds, and which otherwise take default values of 1 for F or 0 for P, R_{O_3}, and Q. The parameter A is a multiplier and γ_S is a variable connected to the VOC's structure.

With this method, the POCPs[39] of VOCs are calculated in relation to ethane, which is given a value of 100. The estimated POCP value for AA is 70.2. It can be observed that, in comparison to ethane as a reference compound, AA has significant risk of contributing to photochemical smog. Furthermore, using the reported[40] Dash *et al.*, 2013 eqn (15), it was estimated the $[O_3]$ during the reaction of VOCs with OH radicals.

$$O_3 = \frac{n'[k_a(OH)]^2}{4.6[2.7 \times 10^{-5} - k(OH)]} \times \left(\frac{1}{k_a(OH)} - \frac{1 - e^{-1.24 \times 10^{-4}/k_a(OH)}}{2.7 \times 10^{-5}}\right) \quad (15)$$

where n' is the maximum possible ozone molecules that can be produced from one molecule of VOC based on the number of $n_C + n_H$ atoms present in that molecule, k_a is the rate coefficient, and (OH) is the global weighted-average OH radical concentration. The average ozone production during the reaction of AA with OH radicals was estimated to be 2.15 ppm. This value can be compared with of ethene value, 3.30 ppm. Due to the close values, the degradation of AA could have a negative impact on human health since it will increase the tropospheric ozone.

The release of AA into the atmosphere can contribute to the overall chemical composition of the air. In small quantities, it is unlikely to have a significant impact on air quality. However, if large amounts of AA are released, either from industrial processes, it can contribute to the formation of secondary pollutants such as ozone or particulate matter. AA can degrade in the atmosphere to produce a number of VOCs with different impacts on the troposphere and the surface of the planet.

Small aldehydes, such as formaldehyde (CH_2O) and acetaldehyde (CH_3CHO), can have atmospheric implications due to their reactivity. These aldehydes are highly reactive compounds in the atmosphere. They can participate in photochemical reactions, reacting with other atmospheric constituents such as hydroxyl radicals (OH) and nitrogen oxides (NO_x).[41,42] These reactions can contribute to the formation of secondary pollutants, including peroxyacetyl nitrates (PANs) and ozone (O_3), which can impact on air quality. Both formaldehyde and acetaldehyde are known to contribute to the formation of ground-level ozone, which are a harmful pollutant and a component of smog. They can also contribute to the formation of secondary organic aerosols, which have implications for air quality and human health. Formaldehyde is classified as a human carcinogen by the International Agency for Research on Cancer (IARC),[43] and it can cause respiratory irritation and other health issues. Acetaldehyde is a respiratory irritant and is also classified as a potential carcinogen. For this reason, numerous field studies are carried out to evaluate the levels of carbonyl VOCs as main pollutants in the atmosphere of populated cities and their potential risk to health.[44,45]

Acetic acid is readily soluble in water, and its fate in the atmosphere depends on various factors such as temperature, humidity, and reaction rates. It can undergo oxidation reactions to form other organic compounds or be scavenged by precipitation and deposited onto the Earth's surface.

5 Conclusions

Once released into the atmosphere, AA can undergo various chemical reactions. It can be degraded by reactions with hydroxyl radicals or other oxidizing agents present in the atmosphere. The exact fate of AA will depend on the specific conditions of the environment, such as the presence of sunlight, other pollutants, and the atmospheric concentrations of reactive species.

The residence time of AA is around 22 hours for reaction with OH radicals and 62 hours in reaction with Cl atoms. It would have a regional and local impact.

The degradation mechanism initiated by the Cl atoms is similar that OH radicals by H-atoms abstraction from the alkyl groups followed by O_2 addition to form the peroxy radicals further alkoxy radical's formation. The fate of alkoxy radicals depends on several reaction pathways.

AA can degrade in the atmosphere to produce a number of VOCs as acetic acid, formaldehyde, acetaldehyde, propionaldehyde, and butyraldehyde with different impacts on the troposphere. Small aldehydes can contribute to produces other pollutants, such as peroxyacetyl nitrates (PANs) and ozone (O_3).

The reaction of OH radicals with AA might have a harmful effect on human health since it will cause the creation of a considerable amount of tropospheric ozone and has a significant risk of contributing to photochemical smog.

Conflicts of interest

There are no conflicts to declare.

Acknowledgements

The authors wish to acknowledge to EUROCHAMP 2020, FONCyT, CONICET and SECyT UNC, Argentina. M. B. B. wish to acknowledge the Alexander von Humboldt Foundation for financial support. V. G. S. C. wishes to acknowledge to CONICET for a doctoral fellowship and support.

References

1 R. Atkinson, Gas-phase tropospheric chemistry of organic compounds: a review, *Atmos. Environ.*, 2007, **41**, 200–240.

2 A. El Boudali, S. Le Calvé, G. Le Bras and A. Mellouki, Kinetic Studies of OH Reactions with a Series of Acetates, *J. Phys. Chem.*, 1996, **100**, 12364–12368.
3 P. Ibanez, 1: Final report on the safety assessment of amyl acetate and isoamyl acetate, *J. Am. Coll. Toxicol.*, 1988, **7**, 705–719.
4 I. Barnes, K. H. Becker and N. Mihalopoulos, An FTIR product study of the photooxidation of dimethyl disulfide, *J. Atmos. Chem.*, 1994, **18**, 267–289.
5 R. Atkinson, D. L. Baulch, R. A. Cox, R. F. Hampson, J. A. Kerr, M. J. Rossi and J. Troe, Evaluated Kinetic, Photochemical and Heterogeneous Data for Atmospheric Chemistry: Supplement V. IUPAC Subcommittee on Gas Kinetic Data Evaluation for Atmospheric Chemistry, *J. Phys. Chem. Ref. Data*, 1997, **26**, 521–1011.
6 A. Bonard, V. Daële, J.-L. Delfau and C. Vovelle, Kinetics of OH Radical Reactions with Methane in the Temperature Range 295–660 K and with Dimethyl Ether and Methyl-*tert*-butyl Ether in the Temperature Range 295–618 K, *J. Phys. Chem. A*, 2002, **106**, 4384–4389.
7 *Evaluated Kinetic and Photochemical Data for Atmospheric Chemistry: Supplement IV: IUPAC Subcommittee on Gas Kinetic Data Evaluation for Atmospheric Chemistry – ScienceDirect*, **https://www.sciencedirect.com/science/article/abs/pii/096016869290383V**, (accessed 17 March 2023).
8 E. C. Tuazon, R. Atkinson, S. M. Aschmann, M. A. Goodman and A. M. Winer, Atmospheric reactions of chloroethenes with the OH radical, *Int. J. Chem. Kinet.*, 1988, **20**, 241–265.
9 R. Atkinson and S. M. Aschmann, Kinetics of the gas-phase reactions of Cl atoms with chloroethenes at 298 ± 2 K and atmospheric pressure, *Int. J. Chem. Kinet.*, 1987, **19**, 1097–1105.
10 O. US EPA, *EPI Suite™-Estimation Program Interface*, **https://www.epa.gov/tsca-screening-tools/epi-suitetm-estimation-program-interface**, (accessed 23 March 2023).
11 E Kwok and R Atkinson, Estimation of hydroxyl radical reaction rate constants for gas-phase organic compounds using a structure-reactivity relationship: An update, *Atmos. Environ.*, 1995, **29**, 1685–1695.
12 D. C. Williams, L. N. O'Rji and D. A. Stone, Kinetics of the reactions of OH radicals with selected acetates and other esters under simulated atmospheric conditions, *Int. J. Chem. Kinet.*, 1993, **25**, 539–548.
13 A. Zogka, Atmospheric Degradation of a Series of Methoxy and Ethoxy Acetates and *n*-Pentyl Acetate, *PhD thesis*, Université d'Orléans, 2016.
14 S. Ifang, T. Benter and I. Barnes, Reactions of Cl atoms with alkyl esters: kinetic, mechanism and atmospheric implications, *Environ. Sci. Pollut. Res.*, 2015, **22**, 4820–4832.
15 L. N. Farrugia, I. Bejan, S. C. Smith, D. J. Medeiros and P. W. Seakins, Revised structure activity parameters derived from new rate coefficient determinations for the reactions of chlorine atoms with a series of seven ketones at 290 K and 1 atm, *Chem. Phys. Lett.*, 2015, **640**, 87–93.
16 S. M. Aschmann and R. Atkinson, Rate constants for the gas-phase reactions of alkanes with Cl atoms at 296 ± 2 K: Gas-Phase reactions of alkanes, *Int. J. Chem. Kinet.*, 1995, **27**, 613–622.
17 J.-H. Xing, K. Takahashi, M. D. Hurley and T. J. Wallington, Kinetics of the reactions of chlorine atoms with a series of acetates, *Chem. Phys. Lett.*, 2009, **474**, 268–272.
18 R. Atkinson, Kinetics and mechanisms of the gas-phase reactions of the hydroxyl radical with organic compounds under atmospheric conditions, *Chem. Rev.*, 1986, **86**, 69–201.
19 G. S. Tyndall, A. S. Pimentel and J. J. Orlando, Temperature Dependence of the Alpha-Ester Rearrangement Reaction, *J. Phys. Chem. A*, 2004, **108**, 6850–6856.
20 B. Picquet, S. Heroux, A. Chebbi, J.-F. Doussin, R. Durand-Jolibois, A. Monod, H. Loirat and P. Carlier, Kinetics of the reactions of OH radicals with some oxygenated volatile organic compounds under simulated atmospheric conditions, *Int. J. Chem. Kinet.*, 1998, **30**, 839–847.
21 C. Ferrari, A. Roche, V. Jacob, P. Foster and P. Baussand, Kinetics of the reaction of OH radicals with a series of esters under simulated conditions at 295 K, *Int. J. Chem. Kinet.*, 1996, **28**, 609–614.
22 M. Veillerot, P. Foster, R. Guillermo and J. C. Galloo, Gas-phase reaction of n-butyl acetate with the hydroxyl radical under simulated tropospheric conditions: relative rate constant and product study, *Int. J. Chem. Kinet.*, 1996, **28**, 235–243.
23 L. K. Christensen, J. C. Ball and T. J. Wallington, Atmospheric Oxidation Mechanism of Methyl Acetate, *J. Phys. Chem. A*, 2000, **104**, 345–351.
24 M. T. Baumgartner, R. A. Taccone, M. A. Teruel and S. I. Lane, Theoretical study of the relative reactivity of chloroethenes with atmospheric oxidants (OH, NO_3, O(3P), Cl(2P) and Br(2P)), *Phys. Chem. Chem. Phys.*, 2002, **4**, 1028–1032.
25 M. B. Blanco, I. Bejan, I. Barnes, P. Wiesen and M. A. Teruel, Temperature-dependent rate coefficients for the reactions of Cl atoms with methyl methacrylate, methyl acrylate and butyl methacrylate at atmospheric pressure, *Atmos. Environ.*, 2009, **43**, 5996–6002.
26 N. Schütze, X. Zhong, S. Kirschbaum, I. Bejan, I. Barnes and T. Benter, Relative kinetic measurements of rate coefficients for the gas-phase reactions of Cl atoms and OH radicals with a series of methyl alkyl esters, *Atmos. Environ.*, 2010, **44**, 5407–5414.
27 S. Le Calvé, G. Le Bras and A. Mellouki, Kinetic Studies of OH Reactions with a Series of Methyl Esters, *J. Phys. Chem. A*, 1997, **101**, 9137–9141.
28 V. F. Andersen, K. B. Ørnsø, S. Jørgensen, O. J. Nielsen and M. S. Johnson, Atmospheric Chemistry of Ethyl Propionate, *J. Phys. Chem. A*, 2012, **116**, 5164–5179.
29 P. M. Cometto, V. Daële, M. Idir, S. I. Lane and A. Mellouki, Reaction Rate Coefficients of OH Radicals and Cl Atoms with Ethyl Propanoate, *n*-Propyl Propanoate, Methy l,2-Methylpropanoate, and Ethyl *n*-Butanoate, *J. Phys. Chem. A*, 2009, **113**, 10745–10752.
30 F. Taketani, Y. Matsumi, T. J. Wallington and M. D. Hurley, Kinetics of the gas phase reactions of chlorine atoms with a series of ketones, *Chem. Phys. Lett.*, 2006, **431**, 257–260.

31 R. Atkinson, S. M. Aschmann, W. P. L. Carter and J. N. Pitts, Rate constants for the gas-phase reaction of OH radicals with a series of ketones at 299 ± 2 K: Reaction of OH radicals and ketones, *Int. J. Chem. Kinet.*, 1982, **14**, 839–847.

32 E. Jiménez, B. Ballesteros, E. Martínez and J. Albaladejo, Tropospheric Reaction of OH with Selected Linear Ketones: Kinetic Studies between 228 and 405 K, *Environ. Sci. Technol.*, 2005, **39**, 814–820.

33 S. Lin and J. March, March's Advanced Organic Chemistry: Reactions, Mechanisms, and Structure, *Molecules*, 2001, **6**, 1064–1065.

34 N. O. of D. and Informatics, *Libro del Web de Química del NIST*, **https://webbook.nist.gov/chemistry/**, (accessed 14 July 2023).

35 M. B. Blanco and M. A. Teruel, Atmospheric degradation of fluoroesters (FESs): gas-phase reactivity study towards OH radicals at 298 K, *Atmos. Environ.*, 2007, **41**, 7330–7338.

36 R. Hein, P. J. Crutzen and M. Heimann, An inverse modeling approach to investigate the global atmospheric methane cycle, *Global Biogeochem. Cycles*, 1997, **11**, 43–76.

37 O. W. Wingenter, M. K. Kubo, N. J. Blake, T. W. Smith Jr., D. R. Blake and F. S. Rowland, Hydrocarbon and halocarbon measurements as photochemical and dynamical indicators of atmospheric hydroxyl, atomic chlorine, and vertical mixing obtained during Lagrangian flights, *J. Geophys. Res.: Atmos.*, 1996, **101**, 4331–4340.

38 S. Langer, E. Ljungström and I. Wängberg, Rates of reaction between the nitrate radical and some aliphatic esters, *J. Chem. Soc., Faraday Trans.*, 1993, **89**, 425–431.

39 M. E. Jenkin, R. G. Derwent and T. J. Wallington, Photochemical ozone creation potentials for volatile organic compounds: rationalization and estimation, *Atmos. Environ.*, 2017, **163**, 128–137.

40 M. R. Dash and B. Rajakumar, Experimental and theoretical rate coefficients for the gas phase reaction of β-Pinene with OH radical, *Atmos. Environ.*, 2013, **79**, 161–171.

41 R. Atkinson, D. L. Baulch, R. A. Cox, J. N. Crowley, R. F. Hampson, R. G. Hynes, M. E. Jenkin, M. J. Rossi and J. Troe, Evaluated kinetic and photochemical data for atmospheric chemistry: volume III gas phase reactions of inorganic halogens, *Atmos. Chem. Phys.*, 2007, **7**, 981–1191.

42 R. Atkinson, C. N. Plum, W. P. L. Carter, A. M. Winer and J. N. Pitts, Rate constants for the gas-phase reactions of nitrate radicals with a series of organics in air at 298 ± 1 K, *J. Phys. Chem.*, 1984, **88**, 1210–1215.

43 IARC, Formaldehyde, 2-Butoxyethanol and 1-*tert*-Butoxypropan-2-ol, *IARC Monogr. Eval. Carcinog. Risks Hum.*, 2006, **88**, 1–497.

44 F. Villanueva, A. Tapia, A. Notario, J. Albaladejo and E. Martínez, Ambient levels and temporal trends of VOCs, including carbonyl compounds, and ozone at Cabañeros National Park border, Spain, *Atmos. Environ.*, 2014, **85**, 256–265.

45 Y.-Y. Lu, Y. Lin, H. Zhang, D. Ding, X. Sun, Q. Huang, L. Lin, Y.-J. Chen, Y.-L. Chi and S. Dong, Evaluation of Volatile Organic Compounds and Carbonyl Compounds Present in the Cabins of Newly Produced, Medium- and Large-Size Coaches in China, *Int. J. Environ. Res. Public Health*, 2016, **13**, 596.